

Modelling the nonlinear mechanical characteristics of a slack cable using Bouc-Wen model

Shima Zamanian Najafabadi*, Alireza Ture Savadkoohi[†] and Sébastien Langlois[‡]

**Civil and Building Engineering Department, University of Sherbrooke, Canada.*

[†]*Univ Lyon, ENTPE, CNRS UMR5513, LTDS, France*

[‡]*Univ Sherbrooke, Civil and Building Engineering Department, Canada.*

Summary. Slack cables are pieces of conductors that are used in bretelles and Stockbridge dampers, to mitigate the wind-induced vibration of overhead transmission lines. Under cyclic and dynamic excitations, inter-strand friction in slack cables makes their behavior nonlinear and hysteretic. On the other hand, due to the low tension, their mechanical behavior is different from stretched cables. Thus, it is important to develop a model that can predict their nonlinear behaviors under vibration. The main purpose of this study is to reproduce this nonlinear behavior using a linear Euler-Bernoulli beam coupled with a Bouc-Wen hysteresis model. The parameters of the Bouc-Wen model are identified based on the results of a characterization test on the slack cable of a Stockbridge damper, available in the literature. Using this method, the local bending behavior of the slack cable is well-reproduced.

Introduction

When a system exhibits hysteresis behavior, it means the response of the system depends not only on its current state, but also on the history of the previous states. Under cyclic loads, friction between the sliding wires of a slack cable makes their mechanical behavior nonlinear and hysteretic. This characteristic is important since it governs the energy dissipation of the system. In contrast to taut cables, the power dissipation of slack cables is significant, and they are used in bretelles and Stockbridge dampers to mitigate the aeolian vibration of overhead transmission lines. Aeolian vibration represents the major cause of fretting fatigue failure in transmission lines [1].

Due to hysteretic characteristics, the bending stiffness of a cable varies according to the curvature. In the literature, there are several models for the study of the nonlinear bending stiffness of taut cables. These models allow for predicting hysteresis load-deflection curves and calculation of the system energy dissipation. The model of Papailiou [2] describes the secants bending stiffness as a function of curvature taking into account the inter-layer slippage and friction force between the layers of a conductor. This model is validated through the results of quasi-static tests for high level of tensions. The bending stiffness was shown to transmit smoothly from EI_{max} to EI_{min} , which corresponds to the full-stick state and full-slip state, by the propagation of the wire slippage layer by layer towards the core. Dastous [3] converted the model of papailiou based on the tangent bending stiffness method and implemented it in a finite-element formulation. Hong [4] improved the model of Papailiou by reconsidering some simplifying assumptions, and introducing new criteria for wire slippage regarding the radial pressure transmission between the layers. Paradis [5] used the criteria of Hong [4], and developed a new model by considering the micro-slips in contact areas between the wires. Langlois [6] implemented the model of Paradis, and reproduced the variable bending stiffness of tensioned conductors through a finite element model.

To study specifically the hysteresis behavior of slack cables, Sauter [7] modeled the messenger cable of a Stockbridge damper as a linear beam coupled with the Masing hysteresis model to describe the local moment-curvature relationship. Parameters of the model were obtained locally, based on the results of quasi-static tests. It was shown that the behavior of the slack cable during the bending process, varies spatially along the cable and during the bending cycle based on the deformation history (loading-unloading). Foti et al. [8] reproduced the hysteresis moment-curvature of a damper cable using a bilinear elastic-plastic model coupled with the classic Bouc-Wen model. Langlois [9], developed a finite-element model of the messenger cable of a Stockbridge damper with variable bending stiffness by superimposing beam elements with material nonlinearity. The constitutive parameters of the model were identified from the characterization test on Stockbridge dampers such that the overall behavior was best reproduced. The model of damper later was added to a span of conductor to study the aeolian vibration amplitude of a system of conductor-damper.

Low tension in slack cables makes their behavior different from tensioned cables, and very few researches are available to study the nonlinear mechanical bending behavior of the slack cables. The main objective of this study is to develop a nonlinear model that predicts the hysteresis behavior of a slack cable under different amplitudes and frequencies. For this purpose, an analytical model of the slack cable by using a linear Euler-Bernoulli beam coupled with a nonlinear Bouc-Wen model is developed. Bouc-Wen model is a hysteresis model that is based on the continuous change of the stiffness with varying displacement, proposed by Bouc [10] and later improved by Wen [11]. The dynamic response of the system under a low-frequency sinusoidal load is obtained and the moment-curvature hysteresis loop at different locations along the slack-cable is calculated. The parameters of the Bouc-Wen model are obtained iteratively to reproduce the results of the characterization test performed by Sauter [7] on a rigidly clamped slack cable of a Stockbridge damper. This model can be coupled with a validated conductor model to predict the aeolian vibration amplitude of the system.

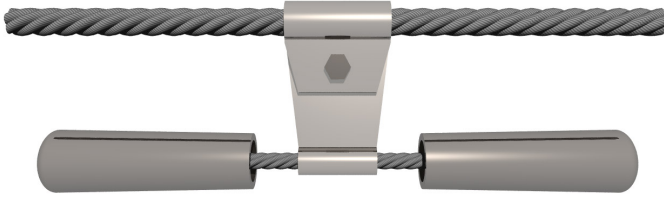


Figure 1: Stockbridge damper [12].

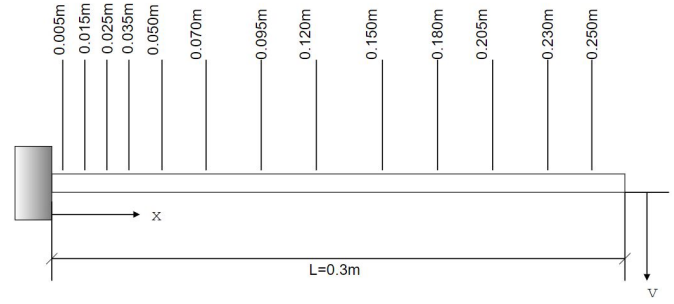


Figure 2: Sketch of the experimental test on the messenger cable.

Properties of the Slack Cable

Slack cables are used in Stockbridge dampers shown in Fig. 1. It consists of a clamp, a short messenger cable, and two inertial masses. This kind of damper is used to mitigate the aeolian vibration of transmission lines. The clamp of the damper is rigidly connected to the conductor, and as the vertical movement of the conductor happens, the masses vibrate and bend the messenger cable. This causes the relative movement of the wires of the messenger cable. Because of the friction between the wires, they exhibit hysteresis behavior. This phenomenon makes the relationship between the load and deflection rate dependent and hence, causes power dissipation in the system. This nonlinearity is shown in the load-deflection curves of messenger cable from experimental tests [13, 14]. Bending tests are usually done to characterize the dissipative behavior of the messenger cables. In these tests, a short length of messenger cable is clamped at one-end and free at the other end, and subjected to a transverse force at the tip monotonically or cyclically varying. The load-deflection curvature curves are usually obtained for different tip displacements.

In this study, the experimental validation of the models are done based on the characterization test of Sauter [7]. In this test, a short slack cable with the length of 0.3 m was rigidly clamp at one-end, and the free-end was subjected to a transverse cyclic displacement at a low frequency. The parameters measured are:

- The moment-curvature diagram at 25mm from the clamp end for cyclic transverse displacement of the free-end (5mm to 30mm peak-peak)
- The local moment-curvature diagram at different points along the cable under the transverse displacement of 25mm peak-peak.

The properties of the slack cable is presented in Table. 1. Figure 2 shows the setup of the test, and the locations for which the local hysteresis were measured.

Governing Equations of the System

In this study, the slack cable is modeled as a simple cantiliver beam (Fig. 2), coupled with a Bouc-wen model. The bending deflection $v(x, t)$ of a Euler-Bernoulli beam under a sinusoidal load $f(t)$ can be described by the following equation:

$$\frac{\partial^2}{\partial x^2} \left(EI(x) \frac{\partial^2 v(x, t)}{\partial x^2} \right) + f(t) = m \frac{\partial^2 v(x, t)}{\partial t^2} + c \frac{\partial v(x, t)}{\partial t} \quad (1)$$

where m is the mass per unit length, c is the damping, EI is the bending stiffness. The boundary conditions for the cantiliver beam are:

$$\begin{aligned} v(0, t) &= 0, \forall t \\ v'(0, t) &= 0, \forall t \\ v''(l, t) &= 0, \forall t \\ v'''(l, t) &= 0, \forall t \end{aligned} \quad (2)$$

Where the prime denotes the derivative with respect to the space variable x , and l is the length of the slack cable.

As we are interested in the behavior of the system around the deformation of its first mode, the solution of the Eq. (1) can be expressed in the form of:

$$v(x, t) = \Gamma_1(x) g_1(t) \quad (3)$$

where $\Gamma_1(x)$ is the first natural mode of the system and $g_1(t)$ is the corresponding generalized coordinate. By solving the eigenvalue problem related to the free response of Eq. (1), the first vibration mode of the beam $\Gamma_1(x)$ could be obtained such that it satisfies the geometrical boundary conditions of the beam presented in Eq. (2).

Table 1: Mechanical Properties of the Slack Cable [7]

Total diameter (mm)	10.15
Number of layers except core	2
Number of wires	19
Wire diameter (mm)	2
Young modulus (GPa)	210
Mass per unit length (kg/m)	0.498

Thanks to the orthogonality of modes, the equation of motion in temporal state after addition of nonlinear Bouc-Wen model could be expressed as [10, 15, 16]:

$$\ddot{g}_1(t) + 2\xi\omega_1\dot{g}_1(t) + \alpha\omega_1^2g_1(t) + (1 - \alpha)\omega_1^2z(t) = F(t) \quad (4)$$

$$\dot{z}(t) = \dot{g}_1(t)[1 - \left|\frac{z(t)}{g_y}\right|^n (\beta + \lambda \operatorname{sgn}(z\dot{g}_1))] \quad (5)$$

Where the dots denotes the derivative with respect to time and ξ is the modal damping ratio, ω_1 is the first angular frequency, $F(t)$ is the modal force and $z(t)$ is the hysteresis parameter. The Bouc-Wen model is coupled with the equation of the beam in temporal state through a superposition of a linear elastic force $\alpha\omega_1^2g_1(t)$ and a nonlinear hysteretic force $(1 - \alpha)\omega_1^2z(t)$. The Bouc-Wen parameters, α is the post-elastic to initial stiffness ratio, g_y is the generalized yield displacement and β , γ , n are model parameters. The response of the system is calculated by direct integration of Eq. (4) and Eq. (5) using "ode45" function in MATLAB. To be able to use this function, the Eq. (4) and Eq. (5) have to be transformed into a system of first order as below:

$$\begin{aligned} \dot{Y}(1) &= Y(2) \\ \dot{Y}(2) &= -2\xi\omega_1Y(2) - \alpha\omega_1^2Y(1) - (1 - \alpha)\omega_1^2Y(3) + F(t) \\ \dot{Y}(3) &= Y(2)[1 - \left|\frac{Y(3)}{g_y}\right|^n (\beta + \lambda \operatorname{sgn}(Y(3)Y(2)))] \end{aligned} \quad (6)$$

The following initial conditions are considered for this system:

$$t = 0 \rightarrow \begin{cases} Y(1) = 0, & \dot{Y}(1) = 0 \\ Y(2) = 0, & \dot{Y}(2) = 0 \end{cases} \quad (7)$$

After obtaining the response of the system numerically, the moment-curvature relationship at each point through the slack cable could be obtained as [17]:

$$M(t) = \alpha\omega_1^2\phi(t) + (1 - \alpha)\omega_1^2z(t) \quad (8)$$

Where $\phi(t)$ is the curvature, and it is calculated directly from the derivative of Eq. (3) with respect to displacement. The moment-curvature diagram is calculated for different excitation loads with a low frequency at the free-end of the slack cable. The force is adjusted to have the desired tip displacements. It has to be noted that this model allows us to predict the behaviour of the system for higher frequencies. The Bouc-Wen parameters of the model are adjusted through an iterative process such that the experimental results is best reproduced.

Model Parameter Identification

The parameters of a messenger cable modeled by the Bouc-Wen model are identified from the experimental data of Sauter [7]. The identification of the model was done iteratively using MATLAB. Five Bouc-Wen parameters, and the local bending stiffness of the system EI are identified. Table 2 shows the identified parameters of the system. Parameters λ and β control the shape and size of the hysteresis loops [11]. α is the post-elastic to initial elastic ratio, and g_y is generalized yield displacement, and the parameter n is a nondimensional number that controls the transition from the elastic to inelastic part of the loop. Increasing this parameter to higher values can sharpen the transition [16]. This value is considered as 1 for all points.

Another parameter that has to be controlled is EI . Bending stiffness of a cable varies significantly with curvature during the bending, however it changes between two limits of EI_{min} and EI_{max} that are related to the full-slip and full-stick states, respectively. These parameters can be calculated as [1]:

$$\begin{aligned} EI_{min} &= \sum_i E_i I_{0i} = 2.83 N.m \\ EI_{max} &= \sum_i E_i (I_{0i} + A_i r_n^2 \sin^2(\alpha_i)) = 67.1 N.m \end{aligned} \quad (9)$$

Table 2: Bouc-Wen parameters of the model

x (m)	α	β	λ	g_y	n
0.005	0.35	45	90	0.06	1
0.015	0.2	45	90	0.05	1
0.025	0.2	45	90	0.0045	1
0.035	0.2	45	90	0.0045	1
0.050	0.19	45	90	0.0045	1
0.070	0.19	45	90	0.0045	1
0.095	0.19	45	90	0.0048	1
0.12	0.19	45	90	0.0049	1
0.15	0.19	45	90	0.007	1
0.18	0.19	45	90	0.008	1
0.205	0.19	45	90	0.008	1
0.230	0.19	45	90	0.009	1
0.250	0.19	45	90	0.008	1

Where E_i is the modulus of elasticity, I_{0i} is the moment of inertia of each wire around its axis, A_i is the area of each wire, r_n is the distance of the center of each wire from the center of the cable, and α_i is the lay angle of each layer. Figure 3 demonstrates the local bending stiffness identified for the slack cable. In this model, the calculated value of EI for the points close to the clamp is more than EI_{max} . The reason could be due to the effect of the clamp on the cable. In the zones far from the clamp, EI decreases to EI_{min} , and from the middle to the tip it remains almost constant. All the wires of the cable far from the clamp slip so fast, however because of clamp effects most of the wires near the clamp stay in stick-state. This explains the variation of the local bending stiffness of the system.

Figures 4-7, show the results obtained from the Bouc-Wen model using the identified parameters (Table. 2) in comparison with experimental results. Figure 4 shows the moment-curvature results of a point 0.025m from the clamp under different tip displacements (5mm to 30mm, each 5mm). Figures 5-7, show the local moment-curvature loops for different points along the cable (Fig. 2) under a constant tip displacement of 25mm. Using the identified parameters, the experimental results are well reproduced in all cases.

As another validation, the displacement of the free end of the cable is measured under a given force. The results are compared to the experimental results in Fig. 8. It should be noted that to compare the global behavior of the slack cable, different sets of identified values are in the Table. 2 are tested, and the values for the point 35mm best reproduced the global behavior. The limitation of this method is that there is no possibility to use different sets of Bouc-Wen parameters at the same time for different points through the beam. However, by selecting a correct sets of values, correct global behavior can be obtained.

Conclusions

The mechanical behavior of a slack cable is modeled using a linear Euler-Bernoulli beam coupled with a hysteresis Bouc-Wen model. In this study, the response of the system is obtained based on the projection of the first mode. The validity of this model is shown by comparing the present results with the experimental results of the slack cable. At both local and global levels, this model reproduced the hysteresis behavior of the slack cable, adequately. The important advantage of this model is providity a fast tool that can describe and predict the nonlinear behavior of the slack cables, without systematic experimental tests. In addition, this model can be integrated into a conductor model, and it allows the assessment of the aeolian vibration amplitude of transmission lines.

References

- [1] EPRI, Transmission Line Reference Book: Wind-Induced Conductor Motion. (2009) Palo Alto, CA, USA: Elect.
- [2] Papailiou K. O. (1997) On the Bending Stiffness of Transmission Line Conductors. *IEEE Power Delivery*. vol. 12, no. 4, pp. 1576–1588.
- [3] Dastous J.-B. (2005) Nonlinear finite-element analysis of stranded conductors with variable bending stiffness using the tangent stiffness method. *IEEE Power Delivery*. vol. 20, no. 1, pp. 328–338.
- [4] Hong K.-J., Kiureghian A. D., and Sackman J. L. (2005) Bending behavior of helically wrapped cables. *ASCE J. Eng. Mechan.*, vol. 131, no. 5, pp. 500–511.
- [5] Paradis JP. H., Legeron F.(2011) Modeling of the Free Bending Behavior of a Multilayer Cable Taking Into Account the Tangential Compliance of Contact Interfaces. *9th Int. Symp. Cable Dynam.*
- [6] Langlois S. (2014) Time History Modeling of Vibrations on Overhead Conductors With Variable Bending Stiffness. *IEEE Power Delivery*. vol. 29, no. 2, pp. 607-614.
- [7] Sauter, D. (2003) Modeling the Dynamic Characteristics of Slack Wire Cables in Stockbridge dampers. *PhD Thesis*, Darmstadt, Germany.
- [8] Foti F. (2018) Hysteretic Behavior of Stockbridge Dampers: Modelling and Parameter Identification. *Mathematical Problems in Engineering*.
- [9] Langlois S. (2014) Prediction of Aeolian Vibration on Transmission-Line Conductors Using a Nonlinear Time History Model—Part I: Damper Model. *IEEE Power Delivery*. 29(3):1176–1183. ISSN 08858977. doi: 10.1109/TPWRD.2013.2291363.
- [10] Bouc R., (1967) Forced Vibration of Mechanical Systems with Hysteresis. *Proceedings of the Fourth Conference on Nonlinear Oscillation*. Prague.

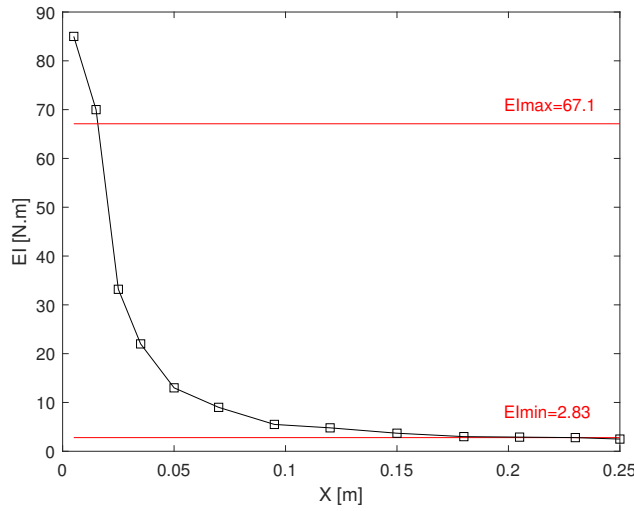


Figure 3: Identified local bending stiffness for the slack cable.

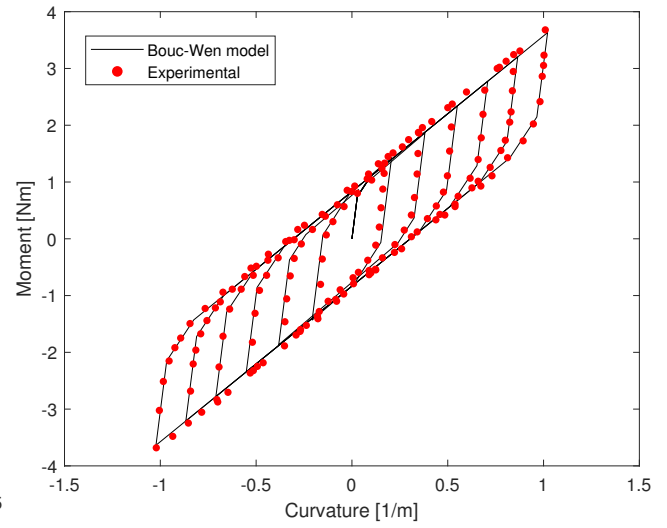


Figure 4: Moment-curvature hysteresis loops at 0.025m from the clamp for end displacement amplitudes (30mm to 5mm).

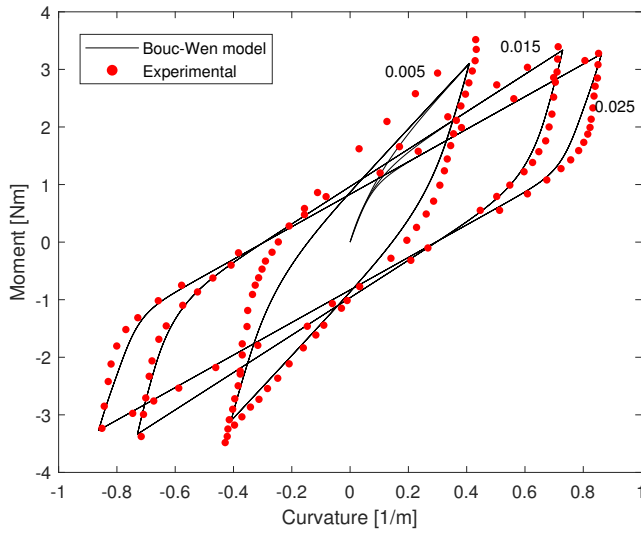


Figure 5: Moment-curvature hysteresis loops for end displacement amplitudes of 25mm at locations 0.005m, 0.015m and 0.025m from the clamp.

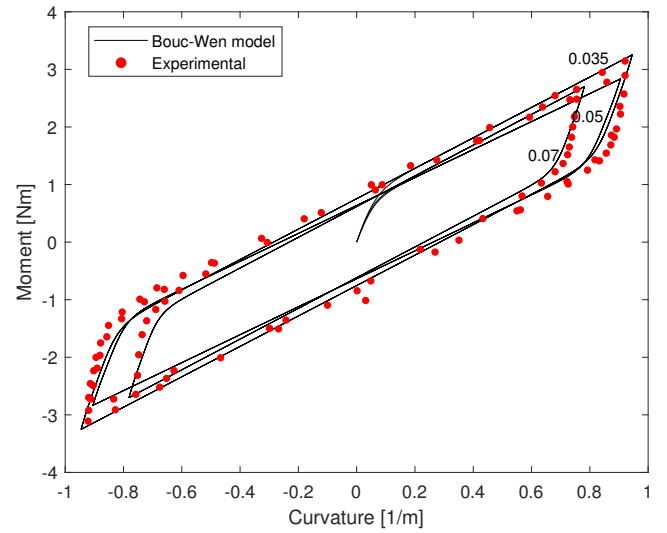


Figure 6: Moment-curvature hysteresis loops for end displacement amplitudes of 25mm at locations 0.035m, 0.05m and 0.07m from the clamp.

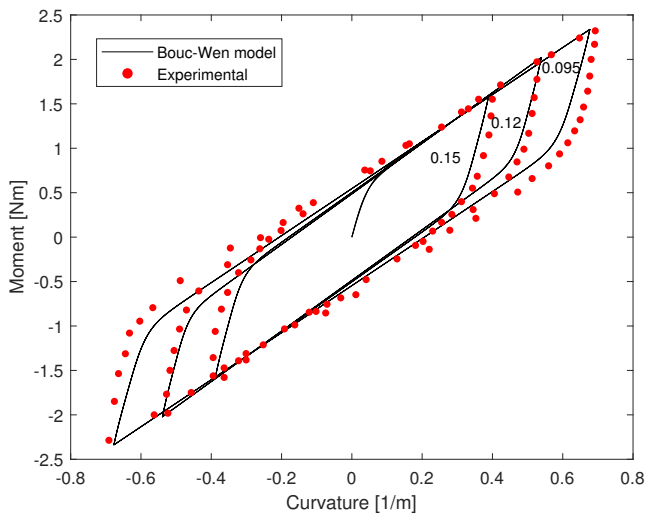


Figure 7: Moment-curvature hysteresis loops for end displacement amplitudes of 25mm at locations 0.095m, 0.12m and 0.15m from the clamp.

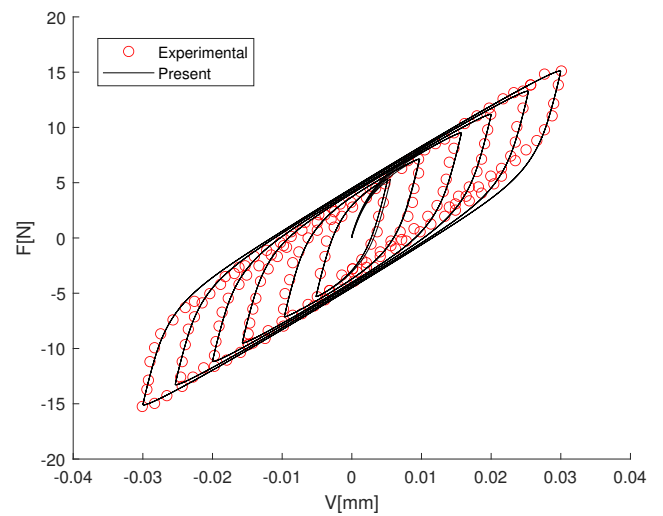


Figure 8: Validation of the force-displacement loops at the tip of the beam.

- [11] Wen, Y.-K.(1980) Equivalent linearization for hysteretic system under random excitation, *Journal of Applied Mechanics*, 47:150-154.
- [12] <https://www.wikidata.org/wiki/Q1713773>.
- [13] Scanlan R. H. and Swart R. L. (1968) Bending stiffness and strain in stranded cables. Presented at the IEEE Winter Power Meeting, New York, Jan.
- [14] Claren R. and Diana G.(1969) Dynamic strain distribution on loaded stranded cables. *IEEE Trans. Power App. Syst.* Vol. PAS-88, no. 11, pp. 1678–1690, Nov.
- [15] Ture Savadkoobi A., Lamarque C. H., (2013) Dynamics of Coupled Dahl Type and Nonsmooth Systems at Different Scales of Time. *International journal of Bifurcation and Chaos*. vol. 23, no. 7, 1350114 (14 pages).
- [16] Ikhoulane F., Rodellar J., (2007) Systems with Hysteresis (John Wiley and Sons).
- [17] Eleni Chatzi, K. Agathos, G. Abbiati (2017) Department of Civil, Environmental, and Geomatic Engineering (DBAUG) ETH Zürich. Lecture Notes: Method of Finite Elements II Modeling of Hysteresis